Structure and stability of trapped atomic boson-fermion mixtures

Robert Roth*

Clarendon Laboratory, University of Oxford, Parks Road, Oxford OX1 3PU, United Kingdom
(Dated: May 8, 2002)

The structure of trapped binary mixtures of bosonic and fermionic atoms at zero temperature is studied using a modified Gross-Pitaevskii equation for the bosons which self-consistently includes the mean-field interaction generated by the fermionic cloud. The density of the fermionic component is described within the Thomas-Fermi approximation. The influence of the boson-boson and the boson-fermion s-wave interaction on the density profiles and the stability of the mixture is investigated systematically. Critical particle numbers for the mean-field collapse caused either by attractive boson-boson or by attractive boson-fermion interactions and for the onset of spatial component separation are discussed. It is shown that the interplay between the boson-boson and the boson-fermion interaction generates a rich and complex phase diagram. Finally, the specific properties and prospects of the boson-fermion mixtures available in present experiments are addressed.

I. INTRODUCTION

Since the first realizations of Bose-Einstein condensation in trapped dilute atomic gases [1] this lively field of research has generated an amount of impressive experimental results illuminating basic quantum phenomena. Besides the studies using bosonic atoms first results were obtained on the cooling of fermionic atoms to a temperature regime where quantum effects dominate the properties of the gas [2, 3]. One of the exciting prospects is the observation of a BCS transition of these degenerate Fermi gases to a superfluid state.

Several successful attempts to trap and cool mixtures of a bosonic and a fermionic species were reported. Quantum degeneracy was first reached with mixtures of bosonic ^{7}Li and fermionic ^{6}Li atoms [4–6]. More recently, experiments to cool mixtures of different atomic elements, i.e. ^{23}Na and ^{6}Li [7] as well as ^{87}Rb and ^{40}K [8, 9], to ultra-low temperatures succeeded. These boson-fermion mixtures offer unique possibilities to study the effects of quantum statistics directly. Besides their interesting physics these systems can be used as an efficient tool to produce a degenerate single-component (spin-polarized) Fermi gas. Direct evaporative cooling is not applicable in a gas of spin-polarized fermions since s-wave interactions are suppressed by the Pauli principle. So the Bose gas, which can be cooled evaporatively, is used as a coolant. The fermionic cloud remains in thermal equilibrium with the cold Bose gas through boson-fermion interactions in the region where both clouds overlap. In this way the fermionic species is cooled sympathetically [10]. Evidently, the shape of the two density distributions as well as their stability are extremely important for the success of the sympathetic cooling scheme.

In this paper I want to investigate systematically the influence of inter-atomic interactions on the structure and stability of binary boson-fermion mixtures at zero temperature. In extension to the work presented in [11] the influence of boson-boson and boson-fermion interactions on the structure of the spatial density distributions and the stability of the system against collapse and phase separation is investigated. All combinations of attractive and repulsive interactions are considered and the implications for present experiments are discussed.

Previous studies of these mixtures mainly rely on the Thomas-Fermi approximation to treat the bosonic component [12, 13]. This restricts the range of applicability significantly; the Thomas-Fermi approximation for the bosonic component is valid only for sufficiently strong repulsive boson-boson interactions and for large boson numbers. Other authors use a variational model, where the bosonic density profile is parameterized by a Gaussian [14, 15]. In many cases this does not provide enough flexibility to describe the density profiles accurately.

To avoid these restrictions from the outset and obtain a model that can be applied for all values of the scattering lengths and for all relevant particle numbers the density of the bosonic component will be obtained from the self-consistent solution of a modified Gross-Pitaevskii equation which is coupled to the fermionic density distribution through the boson-fermion interaction [11, 16]. The fermionic component is treated in Thomas-Fermi approximation which actually is a very good approximation to describe a degenerate Fermi gas [17, 18].

The paper is structured as follows: In Section II the coupled set of differential equations that describes the bosonic and fermionic density distributions is derived and its numerical treatment is discussed. Using this universal tool the generic properties of binary mixtures are investigated in detail in Sections III and IV. Depending on the particle numbers, the boson-boson scattering length, and the boson-fermion scattering length the instability of the mixture against mean-field collapse and spatial component separation is discussed. Finally, in Section V the consequences for the particular boson-fermion mixtures available in present experiments are summarized.

---
*Electronic address: robert.roth@physics.ox.ac.uk

II. MODEL FOR DILUTE BOSON-FERMION MIXTURES

We aim at the description of ground state properties of a dilute mixture of N_B bosonic and N_F fermionic atoms in an external trapping potential at zero temperature. The atoms can be considered as inert interacting bosonic or fermionic particles, because the energy scales involved are sufficiently small, i.e., internal excitations of the atoms are not relevant.

A. Mean-field approximation and effective Hamiltonian

A simple starting point for the treatment of the quantum mechanical many-body problem of $N = N_B + N_F$ interacting bosons and fermions is the mean-field approximation. The many-body state that describes the binary mixture can be written as a direct product of a bosonic N_B-body state $|\Phi_B\rangle$ and a fermionic N_F-body state $|\Psi_F\rangle$

$$|\Psi\rangle = |\Phi_B\rangle \otimes |\Psi_F\rangle. \tag{1}$$

Within the mean-field approximation each of these states is described by a symmetrized or antisymmetrized product of single-particle states. At zero temperature the bosonic state is a direct product of N_B identical single-particle states $|\phi_B\rangle$

$$|\Phi_B\rangle = |\phi_B\rangle \otimes \cdots \otimes |\phi_B\rangle \tag{2}$$

which is symmetric per se. The fermionic state necessarily is a Slater determinant, i.e. an antisymmetrized product of different single-particle states $|\psi_1\rangle, ..., |\psi_{N_F}\rangle$,

$$|\Psi_F\rangle = \boldsymbol{A}\big(|\psi_1\rangle \otimes |\psi_2\rangle \otimes \cdots \otimes |\psi_{N_F}\rangle\big), \tag{3}$$

where $\boldsymbol{A}$ is the antisymmetrization operator.

The mean-field picture is a reasonable starting point as long as correlations induced by the two-body interaction between the constituents are weak. The two-body potential that describes the interaction between the atoms consists of an attractive part at larger particle distances and a strong repulsion at short distances. Especially the short-range repulsion, the so called core, induces strong correlations between the atoms: The probability to find two particles within the range of the core is nearly zero, i.e., the two-body density shows a pronounced hole for particle distances smaller than the radius of the core. Correlations of this kind cannot be described in mean-field approximation.

In order to use the mean-field approximation for the description of the interacting system one has to replace the full atom-atom potential by a suitable effective interaction that contains the relevant physical properties of the the original potential [17]. Since the gases we are considering are extremely dilute and cold the particles do not resolve the detailed shape of the potential. Therefore one may replace the interatomic potential by a simple contact interaction for all partial waves. The strengths of the contact terms are adjusted such that the expectation values of the contact interaction in two-body product states reproduce the two-body energy spectrum of the original atom-atom potential. This leads to a closed form of the effective contact interaction for all partial waves which involves only the scattering lengths of the original potential as discussed in detail in Ref. [17].

Using the effective contact interaction one can set up the Hamiltonian of a binary boson-fermion mixture. It consist of a part $\boldsymbol{H}_B$ that involves only the bosonic component, a part $\boldsymbol{H}_F$ which describes only the fermionic component, and a part $\boldsymbol{H}_{BF}$ which represents the interaction between the two species

$$\boldsymbol{H} = \boldsymbol{H}_B + \boldsymbol{H}_F + \boldsymbol{H}_{BF}. \tag{4}$$

The bosonic part contains the kinetic energy, the external trapping potential $U_B(\vec{x})$ experienced by the bosons, and the s-wave interaction between bosons

$$\begin{aligned}
\boldsymbol{H}_B = \sum_{i=1}^{N} &\left[\frac{\vec{\boldsymbol{p}}_i^2}{2m_B} + U_B(\vec{\boldsymbol{x}}_i)\right] \boldsymbol{\Pi}_i^B \\
&+ \frac{4\pi a_{B0}}{m_B} \sum_{i<j=1}^{N} \delta^{(3)}(\vec{\boldsymbol{r}}_{ij}) \boldsymbol{\Pi}_{ij}^{BB},
\end{aligned} \tag{5}$$

where m_B is the mass of the bosonic atoms and a_{B0} the s-wave scattering length of the boson-boson interaction ($\hbar = 1$ throughout this paper). The formal distinction between bosonic and fermionic atoms is accomplished by projection operators $\boldsymbol{\Pi}_i^B$ and $\boldsymbol{\Pi}_i^F$ onto bosonic and fermionic single-particle states. Accordingly, the two-body projection operators $\boldsymbol{\Pi}_{ij}^{BB}$, $\boldsymbol{\Pi}_{ij}^{FF}$, and $\boldsymbol{\Pi}_{ij}^{BF}$ select pairs of two bosons, pairs of fermions, and boson-fermion pairs, respectively.

The structure of the fermionic part of the Hamiltonian differs from that of the bosonic part: Due to the Pauli principle s-wave contact interactions between identical fermions do not contribute. The lowest order interaction contribution is therefore the p-wave contact interaction, which will be included here. The operator of the p-wave contact interaction is necessarily nonlocal, i.e., it involves the relative momentum operator $\vec{\boldsymbol{q}}_{ij} = \frac{1}{2}(\vec{\boldsymbol{p}}_i - \vec{\boldsymbol{p}}_j)$ of the interacting particle pair. Thus the fermionic Hamiltonian reads

$$\begin{aligned}
\boldsymbol{H}_F = \sum_{i=1}^{N} &\left[\frac{\vec{\boldsymbol{p}}_i^2}{2m_F} + U_F(\vec{\boldsymbol{x}}_i)\right] \boldsymbol{\Pi}_i^F \\
&+ \frac{4\pi a_{F1}^3}{m_F} \sum_{i<j=1}^{N} \vec{\boldsymbol{q}}_{ij}\delta^{(3)}(\vec{\boldsymbol{r}}_{ij})\vec{\boldsymbol{q}}_{ij} \boldsymbol{\Pi}_{ij}^{FF},
\end{aligned} \tag{6}$$

where m_F is the mass of the fermionic atoms, $U_F(\vec{x})$ the respective trapping potential, and a_{F1} the p-wave scattering length [17].

Finally, for the interaction between bosons and fermions, both, s-wave and p-wave terms are present

$$
\begin{aligned}
\boldsymbol{H}_{\mathrm{BF}} =& \frac{4\pi\, a_{\mathrm{BF0}}}{m_{\mathrm{BF}}} \sum_{i<j=1}^{N} \delta^{(3)}(\vec{\boldsymbol{r}}_{ij})\, \boldsymbol{\Pi}_{ij}^{\mathrm{BF}} \\
&+ \frac{4\pi\, a_{\mathrm{BF1}}^3}{m_{\mathrm{BF}}} \sum_{i<j=1}^{N} \vec{\boldsymbol{q}}_{ij}\,\delta^{(3)}(\vec{\boldsymbol{r}}_{ij})\, \vec{\boldsymbol{q}}_{ij}\, \boldsymbol{\Pi}_{ij}^{\mathrm{BF}},
\end{aligned}
\tag{7}
$$

where $m_{\mathrm{BF}} = 2m_{\mathrm{B}}m_{\mathrm{F}}/(m_{\mathrm{B}} + m_{\mathrm{F}})$ is twice the reduced mass of a boson-fermion pair, a_{BF0} is the s-wave, and a_{BF1} the p-wave scattering length of the boson-fermion interaction.

In many cases the p-wave components of the interactions have only a marginal effect because the corresponding p-wave scattering lengths are small. Nevertheless, one can expect a significant influence of p-wave interactions on the structure and stability of the mixture provided the value of the p-wave scattering lengths is in the order of the s-wave scattering lengths or larger, e.g. in the vicinity of a p-wave Feshbach resonance [19]. The strong influence of p-wave interactions on the properties of purely fermionic systems was discussed in detail in Refs. [17, 18].

B. Energy functional

Using the effective Hamiltonian (4) we study the ground state properties of boson-fermion mixtures at zero temperature. I adopt the language of density functional theory and construct, in a first step, an energy functional which connects the energy expectation value of the mixture with the one-body density distributions $n_{\mathrm{B}}(\vec{x})$ and $n_{\mathrm{F}}(\vec{x})$ of the bosons and the fermions, respectively,

$$
\langle\Psi|\,\boldsymbol{H}\,|\Psi\rangle \ \rightarrow\ E[n_{\mathrm{B}}, n_{\mathrm{F}}] = \int\mathrm{d}^3x\, \mathcal{E}(\vec{x}).
\tag{8}
$$

For the construction of the energy functional the different parts of the Hamiltonian (4) are considered separately and the energy density $\mathcal{E}(\vec{x})$ is decomposed into a purely bosonic part $\mathcal{E}_{\mathrm{B}}$, a purely fermionic part $\mathcal{E}_{\mathrm{F}}$, and a part $\mathcal{E}_{\mathrm{BF}}$ that contains the interaction between bosons and fermions

$$
\mathcal{E}(\vec{x}) = \mathcal{E}_{\mathrm{B}}(\vec{x}) + \mathcal{E}_{\mathrm{F}}(\vec{x}) + \mathcal{E}_{\mathrm{BF}}(\vec{x}).
\tag{9}
$$

Using the many-body state (2) the calculation of the expectation value of the bosonic part of the Hamiltonian $\boldsymbol{H}_{\mathrm{B}}$ immediately leads to the well known Gross-Pitaevskii energy density [20]

$$
\begin{aligned}
\mathcal{E}_{\mathrm{B}}(\vec{x}) =& \frac{1}{2m_{\mathrm{B}}}\big|\vec{\nabla}\sqrt{n_{\mathrm{B}}(\vec{x})}\big|^2 + U_{\mathrm{B}}(\vec{x})\, n_{\mathrm{B}}(\vec{x}) \\
&+ \frac{2\pi\, a_{\mathrm{B0}}}{m_{\mathrm{B}}}\, n_{\mathrm{B}}^2(\vec{x}).
\end{aligned}
\tag{10}
$$

The ground state density distribution $n_{\mathrm{B}}(\vec{x})$ of the bosons is connected to the single-particle wave function $\langle\vec{x}|\phi_{\mathrm{B}}\rangle$

in (2) by

$$
n_{\mathrm{B}}(\vec{x}) = \Phi_{\mathrm{B}}^2(\vec{x}) = N_{\mathrm{B}}\,\langle\vec{x}|\phi_{\mathrm{B}}\rangle^2
\tag{11}
$$

which reflects the simple structure of the bosonic part of the many-body state.

For the fermionic part the construction of the associated energy density is not as straight forward. A general treatment of the fermionic many-body problem in mean-field approximation requires the solution of Hartree-Fock equations to obtain the single-particle wave functions [16]. For the experimentally realized particle numbers of $N_{\mathrm{F}} \approx 10^6$ a self-consistent numerical treatment of these differential equations is not feasible. However, the large particle numbers allow the use of the Thomas-Fermi approximation for the fermionic component [17]. It is the lowest order of a semiclassical expansion of the energy density in terms of derivatives of the single-particle density $n_{\mathrm{F}}(\vec{x})$ [21]. All terms in the energy density that involve gradients or higher order derivatives of the density are neglected. To obtain the energy density in Thomas-Fermi approximation one calculates the energy expectation value of the infinite homogeneous system using a Slater determinant of all momentum eigenstates up to the Fermi momentum k_{F} with periodic boundary conditions. Next, one replaces the constant density $n_{\mathrm{F}} = k_{\mathrm{F}}^3/(6\pi^2)$ therein by a density distribution $n_{\mathrm{F}}(\vec{x})$. This leads to the fermionic contribution to the energy density [17, 18]

$$
\begin{aligned}
\mathcal{E}_{\mathrm{F}}(\vec{x}) =& \frac{3(6\pi^2)^{2/3}}{10 m_{\mathrm{F}}}\, n_{\mathrm{F}}^{5/3}(\vec{x}) + U_{\mathrm{F}}(\vec{x})\, n_{\mathrm{F}}(\vec{x}) \\
&+ \frac{(6\pi^2)^{5/3}\, a_{\mathrm{F1}}^3}{5\pi m_{\mathrm{F}}}\, n_{\mathrm{F}}^{8/3}(\vec{x}),
\end{aligned}
\tag{12}
$$

where the first term represents the kinetic energy, the second term the external trapping potential, and the third term the p-wave fermion-fermion interaction.

One can employ the Thomas-Fermi approximation also to calculate the contribution of the boson-fermion interaction to the energy density

$$
\begin{aligned}
\mathcal{E}_{\mathrm{BF}}(\vec{x}) =& \frac{4\pi\, a_{\mathrm{BF0}}}{m_{\mathrm{BF}}}\, n_{\mathrm{B}}(\vec{x}) n_{\mathrm{F}}(\vec{x}) \\
&+ \frac{(6\pi^2)^{5/3} a_{\mathrm{BF1}}^3}{10\pi m_{\mathrm{BF}}}\, n_{\mathrm{B}}(\vec{x}) n_{\mathrm{F}}^{5/3}(\vec{x}),
\end{aligned}
\tag{13}
$$

where the first term describes the s-wave and the second term the p-wave boson-fermion interaction.

Notice that the Thomas-Fermi approximation affects only the contributions to the energy density associated with nonlocal terms of the Hamiltonian, that is the kinetic energy and the p-wave interactions. For fermion numbers in the order $N_{\mathrm{F}} \approx 1000$ one can check explicitly that the Thomas-Fermi approximation is in good agreement with Hartree-Fock type calculations [16]. Alternatively one can evaluate the next terms of the semiclassical gradient expansion of the energy density [17]. Both checks show that the Thomas-Fermi approximation generally yields a very good description of the fermionic component for $N_{\mathrm{F}} \gtrsim 1000$.

Some authors [12, 13] investigated the structure of boson-fermion mixtures using the Thomas-Fermi approximation also for the bosonic species. Here, however, one encounters the problem that the kinetic energy contribution of the bosons vanishes completely (not so for the kinetic energy of the fermions). This causes two stringent conditions for the applicability of the approximation: (a) the boson-boson interaction has to be repulsive, i.e., systems with vanishing or attractive boson-boson interaction cannot be considered at all. (b) The contribution of the boson-boson interaction to the energy density has to be much larger than the neglected kinetic energy. For the investigation of the phase diagram as presented in the following sections this means a substantial and uncontrolled limitation of the parameter range in which the approximation may be valid [11]. Therefore, I employ the Thomas-Fermi approximation only for the fermionic component, where it is well suited for all types of interactions, and treat the bosons using the full Gross-Pitaevskii energy density.

C. Euler-Lagrange equations

The second step is the minimization of the total energy $E[n_{\mathrm{B}}, n_{\mathrm{F}}]$ by functional variation of the boson and fermion density distribution. The variation shall be performed under the constraint of given numbers of bosons and fermions, N_{B} and N_{F}. The constraints are implemented by two Lagrange multipliers, i.e. the chemical potentials μ_{B} and μ_{F}, and an unrestricted variation is carried out for the Legendre transformed energy

$$
\begin{aligned}
F[n_{\mathrm{B}}, n_{\mathrm{F}}] &= E[n_{\mathrm{B}}, n_{\mathrm{F}}] - \mu_{\mathrm{B}} N[n_{\mathrm{B}}] - \mu_{\mathrm{F}} N[n_{\mathrm{F}}] \\
&= \int \mathrm{d}^3 x\, \mathcal{F}(\vec{x})
\end{aligned}
\tag{14}
$$

with a transformed energy density

$$
\mathcal{F}(\vec{x}) = \mathcal{E}(\vec{x}) - \mu_{\mathrm{B}} n_{\mathrm{B}}(\vec{x}) - \mu_{\mathrm{F}} n_{\mathrm{F}}(\vec{x}). \tag{15}
$$

The values of the chemical potentials are chosen (a posteriori) such that the integrals over the boson ($\xi = \mathrm{B}$) and the fermion densities ($\xi = \mathrm{F}$)

$$
N[n_\xi] = \int \mathrm{d}^3 x\, n_\xi(\vec{x}) \tag{16}
$$

yield the desired particle numbers N_{B} and N_{F}, respectively.

A necessary condition for the density distributions $n_{\mathrm{B}}(\vec{x}) = \Phi_{\mathrm{B}}^2(\vec{x})$ and $n_{\mathrm{F}}(\vec{x})$ to describe a minimum of the transformed energy $F[n_{\mathrm{B}}, n_{\mathrm{F}}]$ is given by the Euler-Lagrange equations

$$
0 = \frac{\partial \mathcal{F}}{\partial \Phi_{\mathrm{B}}} - \vec{\nabla} \frac{\partial \mathcal{F}}{\partial(\vec{\nabla}\Phi_{\mathrm{B}})}, \quad 0 = \frac{\partial \mathcal{F}}{\partial n_{\mathrm{F}}} - \vec{\nabla} \frac{\partial \mathcal{F}}{\partial(\vec{\nabla} n_{\mathrm{F}})}. \tag{17}
$$

One can insert the explicit form of $\mathcal{F}(\vec{x})$, which involves the energy densities (10), (12), and (13), and obtain two coupled equations that determine the ground state densities $n_{\mathrm{B}}(\vec{x})$ and $n_{\mathrm{F}}(\vec{x})$.

The Euler-Lagrange equation for the boson density reduces to a modified Gross-Pitaevskii equation

$$
\begin{aligned}
0 = \Bigg[&-\frac{1}{2m_{\mathrm{B}}} \vec{\nabla}^2 + U_{\mathrm{B}}(\vec{x}) - \mu_{\mathrm{B}} + \frac{4\pi\, a_{\mathrm{B}0}}{m_{\mathrm{B}}} \Phi_{\mathrm{B}}^2(\vec{x}) \\
&+ \frac{4\pi\, a_{\mathrm{BF}0}}{m_{\mathrm{BF}}} n_{\mathrm{F}}(\vec{x}) + \frac{(6\pi^2)^{5/3} a_{\mathrm{BF}1}^3}{10\pi m_{\mathrm{BF}}} n_{\mathrm{F}}^{5/3}(\vec{x}) \Bigg] \Phi_{\mathrm{B}}(\vec{x}).
\end{aligned}
\tag{18}
$$

In addition to the usual terms describing kinetic energy, trapping potential, chemical potential, and boson-boson interaction one obtains two contributions from the s- and p-wave interaction between bosons and fermions. The bosons thus experience additional mean-field potentials generated by the boson-fermion interactions that depend on different powers of the fermionic density distribution.

For the fermions the Euler-Lagrange equation simplifies to a polynomial equation in $n_{\mathrm{F}}(\vec{x})$ because all terms in the energy density that involve the fermion density are local — a direct consequence of the Thomas-Fermi approximation

$$
\begin{aligned}
0 = &\left[U_{\mathrm{F}}(\vec{x}) - \mu_{\mathrm{F}} + \frac{4\pi a_{\mathrm{BF}0}}{m_{\mathrm{BF}}} n_{\mathrm{B}}(\vec{x}) \right] \\
&+ \left[\frac{(6\pi^2)^{2/3}}{2m_{\mathrm{F}}} + \frac{(6\pi^2)^{5/3} a_{\mathrm{BF}1}^3}{6\pi m_{\mathrm{BF}}} n_{\mathrm{B}}(\vec{x}) \right] n_{\mathrm{F}}^{2/3}(\vec{x}) \\
&+ \left[\frac{8(6\pi^2)^{5/3} a_{\mathrm{F}1}^3}{15\pi m_{\mathrm{F}}} \right] n_{\mathrm{F}}^{5/3}(\vec{x}).
\end{aligned}
\tag{19}
$$

Again the boson density enters explicitly through the s- and p-wave boson-fermion interaction. The simultaneous solution of Eqs. (18) and (19) yields density profiles that describe a stationary point of the energy functional $F[n_{\mathrm{B}}, n_{\mathrm{F}}]$. In principle one has to check explicitly that these coincide with a minimum of the energy.

D. Numerical treatment

On the basis of the coupled equations (18) and (19) the structure of binary boson-fermion mixtures is studied with special emphasis on the effects and the interplay between the boson-boson and the boson-fermion s-wave interaction.

In order to reduce the number of physical parameters it is assumed that the p-wave scattering lengths are small and the corresponding p-wave terms are neglected. Thus the Euler-Lagrange equations for the boson and fermion density simplify to

$$
\begin{aligned}
0 = \Bigg[&-\frac{1}{2m_{\mathrm{B}}} \vec{\nabla}^2 + U_{\mathrm{B}}(\vec{x}) - \mu_{\mathrm{B}} + \frac{4\pi\, a_{\mathrm{B}}}{m_{\mathrm{B}}} \Phi_{\mathrm{B}}^2(\vec{x}) \\
&+ \frac{4\pi\, a_{\mathrm{BF}}}{m_{\mathrm{BF}}} n_{\mathrm{F}}(\vec{x}) \Bigg] \Phi_{\mathrm{B}}(\vec{x})
\end{aligned}
\tag{20}
$$

for the boson density $n_{\mathrm{B}}(\vec{x}) = \Phi_{\mathrm{B}}^2(\vec{x})$ and

$$n_{\mathrm{F}}(\vec{x}) = \frac{(2m_{\mathrm{F}})^{3/2}}{6\pi^2} \left[\mu_{\mathrm{F}} - U_{\mathrm{F}}(\vec{x}) - \frac{4\pi\, a_{\mathrm{BF}}}{m_{\mathrm{BF}}} n_{\mathrm{B}}(\vec{x}) \right]^{3/2} \quad (21)$$

for the fermion density. The index "0" which marked the s-wave scattering lengths is omitted here and in the following. Furthermore, we will restrict ourselves to parabolic trapping potentials with spherical symmetry

$$U_\xi(\vec{x}) = \frac{m_\xi \omega_\xi^2}{2} x^2 = \frac{1}{2 m_\xi \ell_\xi^4} x^2, \quad (22)$$

where ω_ξ is the oscillator frequency and $\ell_\xi = (m_\xi \omega_\xi)^{-1/2}$ is the corresponding oscillator length for the bosonic ($\xi = \mathrm{B}$) and fermionic component ($\xi = \mathrm{F}$), respectively. In a magnetic trap the trap parameters of the fermionic species can be obtained from those for the bosons by scaling according to the different masses and magnetic moments.

For the numerical treatment it is convenient to express all quantities with the dimension of length in units of the oscillator length ℓ_B and energies in units of the oscillator frequency ω_{B}. Eventually, the physically relevant dimensionless parameters to characterize the mixture are the particle numbers N_{B} and N_{F}, the ratios of the scattering lengths and the oscillator length $a_{\mathrm{B}}/\ell_{\mathrm{B}}$ and $a_{\mathrm{BF}}/\ell_{\mathrm{B}}$, and the ratios of the masses $m_{\mathrm{B}}/m_{\mathrm{F}}$ and of the oscillator lengths $\ell_{\mathrm{B}}/\ell_{\mathrm{F}}$.

The solution of the coupled equations (20) and (21) is accomplished by an efficient imaginary time propagation algorithm — also known as quantum diffusion algorithm [22] — which is embedded in a simple iterative scheme. A basic iteration step consists of two stages: (a) The fermionic density profile $n_{\mathrm{F}}(\vec{x})$ is calculated from (21) with a chemical potential μ_{F} adjusted such that the desired fermion number N_{F} is reproduced. (b) A single imaginary time step is performed using the mean-fields associated with the fermion density determined before and the boson density of the previous iteration step. The resulting $n_{\mathrm{B}}(\vec{x})$ is then normalized to the total boson number N_{B} and used as initialization for the next iteration step. In the beginning of the iteration cycle the boson density is initialized with a Gaussian profile chosen, e.g., according to a variational treatment of the isolated bosonic system.

Typically 200 grid points are used to set up a radial lattice in the region where the bosonic and the fermionic density distributions overlap. The fermionic density profile outside the overlap region (where $n_{\mathrm{B}}(\vec{x}) \equiv 0$) is described using the analytic form (21). The imaginary time propagation itself is implemented using either a linearized time-evolution operator with a simple three-point discretization of the radial part of the Laplacian or by a split operator technique employing a fast Fourier transformation. The size of a time step is chosen sufficiently small to guarantee the stability of the algorithm and the independence of the results. The convergence of the density profiles is monitored during the evolution.

III. ATTRACTIVE BOSON-FERMION INTERACTIONS

In this section generic properties of binary boson-fermion mixture with attractive interactions between the two species ($a_{\mathrm{BF}} < 0$) are discussed. Recent experiments indicate that mixtures of bosonic ^{87}Rb and fermionic ^{40}K atoms belong to this class of interactions [8, 9, 23].

Throughout this and the following section it is assumed that the masses ($m = m_{\mathrm{B}} = m_{\mathrm{F}}$) and the oscillator lengths of the trapping potentials ($\ell = \ell_{\mathrm{B}} = \ell_{\mathrm{F}}$) are identical for both components in order to reduce the parameter manifold to a tractable size.

A. Density profiles

Some of the basic properties of mixtures with attractive boson-fermion interactions become evident from the shape of the density profiles already. Figure 1 shows the radial density profiles for mixtures with $N_{\mathrm{B}} = N_{\mathrm{F}} = 10^4$, $a_{\mathrm{B}}/\ell = 0$, and different strengths of the attractive boson-fermion interaction. Already the noninteracting case $a_{\mathrm{BF}}/\ell = 0$ (solid tlines) reveals a fundamental property of these mixtures: The fermionic density distribution has a much larger spatial extension than a bosonic distribution with the same particle number. This is a direct consequence of the Pauli principle that forces the fermions to occupy "excited" single-particle states of the external potential which have a larger radial extension whereas the bosons in a Bose-Einstein condensate all occupy the ground state of the trap. This manifestation of the so-called Fermi pressure was observed experimentally [4].

The inclusion of an attractive boson-fermion interaction leads to an enhancement of the boson and the fermion density within the central overlap region as it is shown by the broken curves in Fig. 1. The bosonic profile narrows and the central density increases moderately. The effect on the fermionic component is more pronounced: within the overlap region the fermion density exhibits a high-density bump on top of the low-density profile. The central fermion density can easily be increased by a factor of four (dotted line in Fig. 1). This structure can be understood by considering the mean-field potential experienced by the fermions: In addition to a shallow trapping potential the boson-fermion attraction generates a tight potential well with the shape of the bosonic density distribution which causes a localized enhancement of the fermion density profile.

The boson-boson interaction has a strong influence on this density enhancement. The presence of a boson-boson repulsion broadens the bosonic distribution and reduces the maximum density significantly. This in turn strongly reduces the enhancement of the fermion density in the overlap region. As is shown in Fig. 2 much stronger boson-fermion attractions are required to generate a similar increase of the fermion density in the presence of repulsive boson-boson interactions. However, the over-
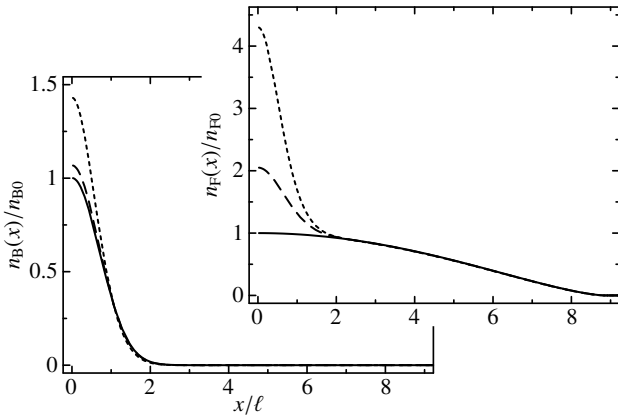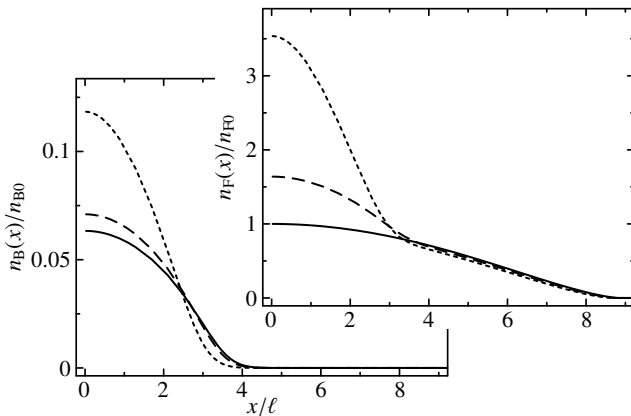
FIG. 1: Boson (lower panel) and fermion density profiles (upper panel) for a mixture with $N_B = N_F = 10^4$ and $a_B/\ell = 0$ for different values of the boson-fermion scattering length: $a_{BF}/\ell = 0.0$ (solid lines), -0.001 (dashed), and -0.002 (dotted). Both densities are given in units of the respective central densities $n_{B0} = N_B/(\pi^{3/2}\ell^3) \approx 1796\,\ell^{-3}$ and $n_{F0} = (48N_F)^{1/2}/(6\pi^2\ell^3) \approx 11.7\,\ell^{-3}$ of the noninteracting system with the same particle numbers.

FIG. 2: Boson and fermion density profiles for a mixture with $N_B = N_F = 10^4$ and $a_B/\ell = 0.005$ for different values of the boson-fermion scattering length: $a_{BF}/\ell = 0.0$ (solid lines), -0.01 (dashed), and -0.02 (dotted). The densities are given in units of the central boson and fermion density of the non-interacting system (compare Fig. 1).

lap volume is much larger in these cases; thus a larger fraction of the fermions is contained in the high-density region.

B. Simultaneous mean-field collapse

For given particle numbers N_B and N_F and given boson-boson scattering length a_B there exists a maximum strength of the attractive boson-fermion interaction up to which the mixture is stable. Physically this stability limit is governed by the balance between the kinetic energy of bosons and fermions and the mutually attractive mean-

field generated by the boson-fermion interaction. If the boson-fermion attraction becomes too strong — likewise if the boson or fermion numbers become too large — the attractive mean-field cannot be stabilized by the kinetic energy anymore and the mixture can lower its energy by increasing the boson and fermion density; both density distributions collapse simultaneously within the overlap region.

In the numerical treatment of the coupled Gross-Pitaevskii problem the instability is indicated by a divergence of the central boson and fermion density during the imaginary time propagation. By monitoring the central density one can determine whether the systems is stable or collapses, i.e., whether the density converges or diverges for a given set of parameters N_B, N_F, a_B/ℓ, and a_{BF}/ℓ. To determine the stability limit in presence of attractive boson-fermion interactions it is most useful to vary a_{BF}/ℓ for fixed values of N_B, N_F, and a_B/ℓ until the onset of instability is reached.

Figure 3 depicts the resulting stability limit in terms of a critical number of bosons N_B^{cr} as function of $a_{BF}/\ell < 0$ for different a_B/ℓ and N_F. To obtain the curves I determined the limiting value of a_{BF}/ℓ that still allows a stable mixture for a set of boson numbers $\log_{10} N_B = 1.5, ..., 6$. The maximum strength of the boson-fermion interaction of $a_{BF}/\ell = -0.05$ shown in the plots corresponds to a scattering length of $a_{BF} \approx -1000\,a_{Bohr} \approx -50\,\text{nm}$ for a typical trap with $\ell = 1\,\mu\text{m}$.

The full curves in Fig. 3 show the critical boson number for a mixture with vanishing boson-boson interaction ($a_B/\ell = 0$). Already a moderate boson-fermion attraction with $a_{BF}/\ell = -0.005$ causes a severe limitation of the boson number to $N_B \lesssim 2300$ in the presence of $N_F = 10^5$ fermions, as it is shown in panel (b) of Fig. 3.

The boson-boson interaction has a very strong influence on the structure and stability of the mixture. If a weak boson-boson repulsion with a fraction of the strength of the boson-fermion attraction is included the system is stabilized significantly, i.e., the critical number of boson N_B^{cr} is increased. This is depicted by the broken curves in Fig. 3 which correspond to different strengths $a_B/\ell > 0$ of the repulsive boson-boson interaction. For the previous example ($a_{BF}/\ell = -0.005$, $N_F = 10^5$) a boson-boson repulsion with $a_B/\ell = 0.001$ is sufficient to increase the maximum number of bosons in a stable system from $N_B^{cr} \approx 2300$ for $a_B/\ell = 0$ to far more than 10^6. Moreover, repulsive boson-boson interactions can cause the absolute stabilization of the mixture against collapse induced by the boson-fermion attraction. That is, for given $a_B/\ell > 0$ and N_F mixtures with $|a_{BF}/\ell|$ below a certain limiting strength are stable up to any number of bosons. This can be clearly seen in Fig. 3(a): the broken thick curves exhibit a kink and start to rise vertically at a specific value of a_{BF}/ℓ which depends on a_B/ℓ and N_F. All systems with weaker boson-fermion attraction are stable against collapse for arbitrary N_B.

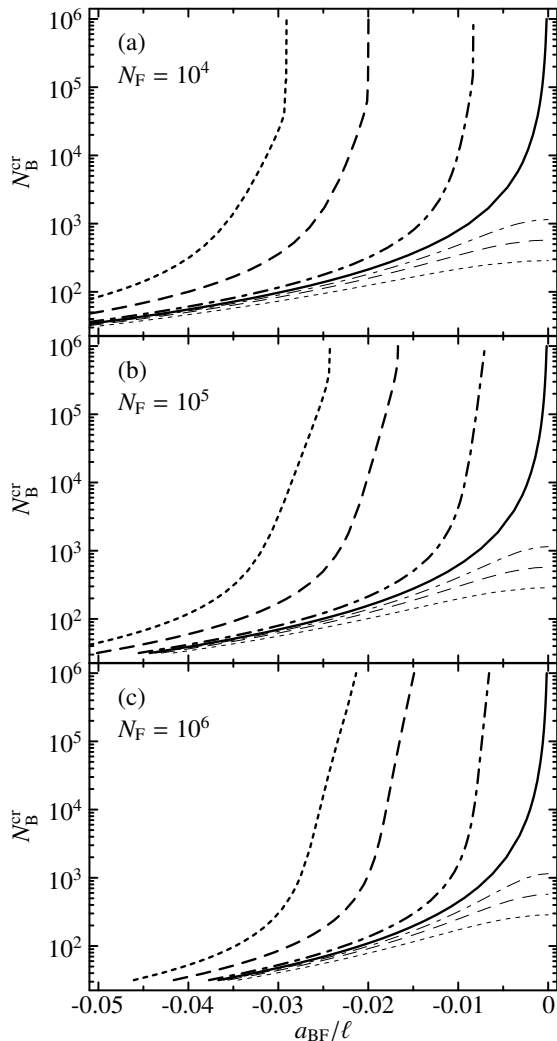An attractive boson-boson interaction, on the other hand, promotes the collapse of the mixture. It generates

FIG. 3: Critical number of bosons $N_{\mathrm{B}}^{\mathrm{cr}}$ above which the mixture collapses simultaneously as function of $a_{\mathrm{BF}}/\ell < 0$. The thick curves correspond to repulsive boson-boson interactions: $a_{\mathrm{B}}/\ell = 0$ (full line), 0.001 (dash-dotted), 0.005 (dashed), 0.01 (dotted). Thin lines show attractive boson-boson interactions: $a_{\mathrm{B}}/\ell = -0.0005$ (thin dash-dotted), -0.001 (thin dashed), -0.002 (thin dotted). The three panels represent different fermion numbers: (a) $N_{\mathrm{F}} = 10^4$, (b) $N_{\mathrm{F}} = 10^5$, (c) $N_{\mathrm{F}} = 10^6$.

an additional attractive contribution to the mean-field experienced by the bosons which seeks to increase the boson density and has to be balanced by the kinetic energy. Due to the boson-fermion attraction the fermionic component in turn feels a stronger mean-field attraction cause by the increased boson density. Therefore the critical boson number $N_{\mathrm{B}}^{\mathrm{cr}}$ is lowered by attractive boson-boson interactions as the thin curves in Fig. 3 show. One has to be aware that the character of the collapse changes if one reduces $a_{\mathrm{BF}}/\ell \to 0$ for fixed $a_{\mathrm{B}}/\ell < 0$. For reasonably strong boson-fermion attraction the mutual mean-field couples the boson and fermion density strongly to each other such that both densities collapse simultaneously in the overlap region. If the boson-fermion

interaction is reduced this coupling weakens until bosons and fermions decouple for $a_{\mathrm{BF}}/\ell = 0$. In this case the boson density may still collapse due to the boson-boson attraction; the fermion density, however, is not affected and remains stable (see also Sec. IV C).

The number of fermions in the system has a rather weak influence on the stability. The three panels in Fig. 3 correspond to (a) $N_{\mathrm{F}} = 10^4$, (b) $N_{\mathrm{F}} = 10^5$, and (c) $N_{\mathrm{F}} = 10^6$. Mainly, the increasing number of fermions N_{F} enhances the effect of the boson-fermion attraction. Thus the stability limit for a given N_{B} is shifted towards smaller values of a_{BF}/ℓ if N_{F} is increased.

IV. REPULSIVE BOSON-FERMION INTERACTIONS

In this section the generic properties of boson-fermion mixtures with repulsive interactions between the two species ($a_{\mathrm{BF}} > 0$) are discussed. All ^{7}Li-^{6}Li mixtures used in present experiments [4–6] belong to this class of interactions.

A. Density profiles

Obviously a repulsive boson-fermion interaction will tend to reduce the overlap between the two species — in contrary to the attractive boson-fermion interactions discussed in the previous section. Hence the structural transition characteristic for this class of interactions is the spatial separation (or demixing) of the two species [12, 16]. Figure 4 shows an example for the influence of repulsive boson-fermion interactions of increasing strength on the density profiles of the mixture. The compact boson distribution in the trap center repels the fermionic cloud from the overlap region. With increasing boson-fermion scattering length $a_{\mathrm{BF}}/\ell > 0$ the fermionic distribution gets more and more depleted until $n_{\mathrm{F}}(\vec{x} = 0)$ reaches zero (see the dashed curve in Fig. 4). For even larger a_{BF}/ℓ the fermions are expelled farther from the trap center and the overlap of both species is reduced continuously. The boson cloud in return is slightly compressed by the outer shell of fermions.

The boson-boson interaction has a very strong influence on the density profiles of bosons and fermions. Similar to the case discussed in Sec. III A a repulsive boson-boson interaction reduces the influence of the boson-fermion interaction. Much larger boson-fermion scattering lengths are required to cause phase separation in the presence of repulsive boson-boson interactions. An example with $a_{\mathrm{B}}/\ell = 0.005$ is shown in Fig. 5. Because the bosonic distribution is broadened due to the boson-boson repulsion, the fermion density is depleted in a significantly larger volume. A peculiar structure appears for interactions with $a_{\mathrm{B}}/\ell = a_{\mathrm{BF}}/\ell > 0$: The fermion density is nearly constant within the whole overlap region as the dash-dotted curve in Fig. 5 shows [12].
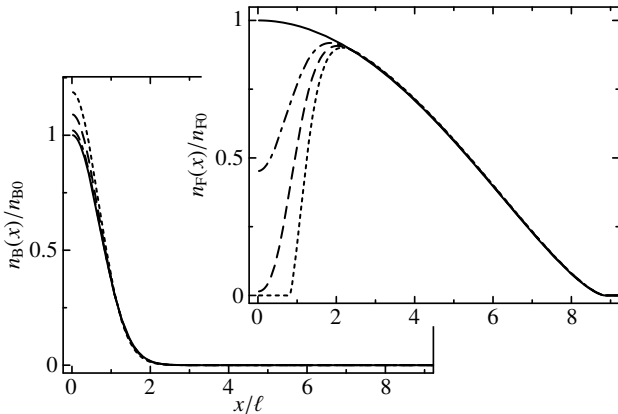
FIG. 4: Boson (lower panel) and fermion density profiles (upper panel) for a mixture with $N_B = N_F = 10^4$ and $a_B/\ell = 0$ for different values of the boson-fermion scattering length: $a_{BF}/\ell = 0.0$ (solid lines), 0.0007 (dash-dotted), 0.0015 (dashed), and 0.003 (dotted). Both densities are given in units of the central densities of the corresponding noninteracting system as in Fig. 1.
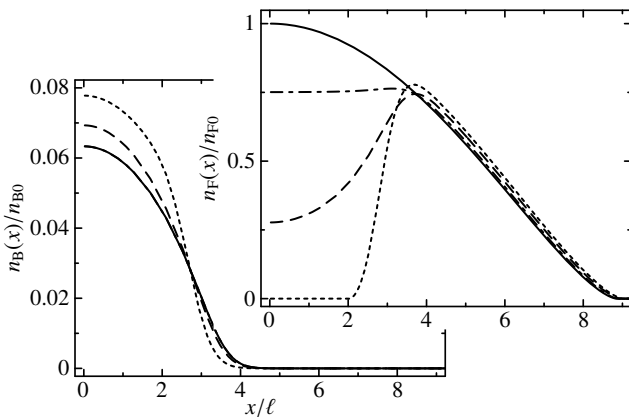

FIG. 5: Boson (lower panel) and fermion density profiles (upper panel) for a mixture with $N_B = N_F = 10^4$ and $a_B/\ell = 0.005$ for different values of the boson-fermion scattering length: $a_{BF}/\ell = 0.0$ (solid lines), 0.005 (dash-dotted), 0.015 (dashed), and 0.03 (dotted). The densities are given in units of the central densities n_{B0} and n_{F0}, resp., of the noninteracting system with the same particle numbers (compare to Fig. 1). The dash-dotted curve for the boson density is on top of the solid curve.

Depending on the trap geometry the separated phase can exhibit different structures. If the fermionic species experiences a tighter confinement than the bosonic component (requires an appropriate combination of magnetic moments) an inversion of the separated configuration can appear: a central core of fermions surrounded by a thin boson shell which compresses the fermions. In these cases there exists a second structural transition from the fermion-core configuration at smaller N_B to the usual boson-core configuration at large N_B. In deformed traps a rich variety of asymmetric configurations are possible,

some of these were discussed in [16].

B. Spatial component separation

In this section the influence of scattering lengths and particle numbers on the transition from overlapping to separated density distributions is quantified. Since the transition is smooth in most cases there is no unique definition for the onset of separation. As a gross criterion for separation I use the fermion density in the trap center and consider those configurations as separated that yield $n_F(\vec{x} = 0) = 0$. Clearly, if the boson-fermion repulsion is increased then the overlap of the two density distributions decreases further.

Figure 6 summarizes the findings on the characteristic number of bosons N_B^{sep} above which the fermion density vanishes in the trap center. The curves correspond to different values of the boson-boson scattering length a_B/ℓ. For increasing boson-fermion repulsion $a_{BF}/\ell > 0$ the characteristic boson number N_B^{sep} drops rapidly. In the case $a_B/\ell = 0$ (solid lines) and $N_F = 10^5$ a moderate boson-fermion repulsion with $a_{BF}/\ell = 0.005$ leads to phase separation if the number of bosons exceeds $N_B^{sep} \approx 3300$.

The inclusion of repulsive boson-boson interactions leads to an interesting modification of the separation behavior. First of all the boson-boson repulsion stabilizes the mixture against phase separation, i.e., N_B^{sep} increases significantly with increasing $a_B/\ell > 0$ as the broken curves in Fig. 6 indicate. Moreover, for sufficiently large fermion numbers the boson-boson repulsion causes a qualitative change of the dependence of N_B^{sep} on the boson-fermion scattering length. An example is shown in Fig. 6(c) for $N_F = 10^6$. Around a characteristic value of a_{BF}/ℓ, which increases with increasing a_B/ℓ, the limiting boson number for separation N_B^{sep} suddenly drops by one or more orders of magnitude and a steplike structure appears. For values of a_{BF}/ℓ smaller than the characteristic value associated with this step the boson-boson repulsion causes a substantial stabilization of the system against separation. Above the step the influence of the boson-boson repulsion on N_B^{sep} is weak.

In addition to the particular behavior of N_B^{sep} the character of the transition changes. One may regard the central fermion density $n_F(0)$ as order parameter; finite values of the order parameter characterize the overlapping phase, a vanishing order parameter indicates separation. In most cases, e.g. for $a_B/\ell = 0$, the order parameter decreases continuously with increasing N_B, i.e., the central fermion density decreases smoothly until the separated phase with $n_F(0) = 0$ is reached. This behavior corresponds to a second order or cross-over transition. However, for sufficiently large N_F and a_B/ℓ, e.g., $N_F = 10^6$ and $a_B/\ell = 0.005$ [see dotted curve in Fig. 6(c)], the order of the phase transition changes. For values of a_{BF}/ℓ above the step the transition is of first order: With increasing N_B the order parameter decreases slightly until
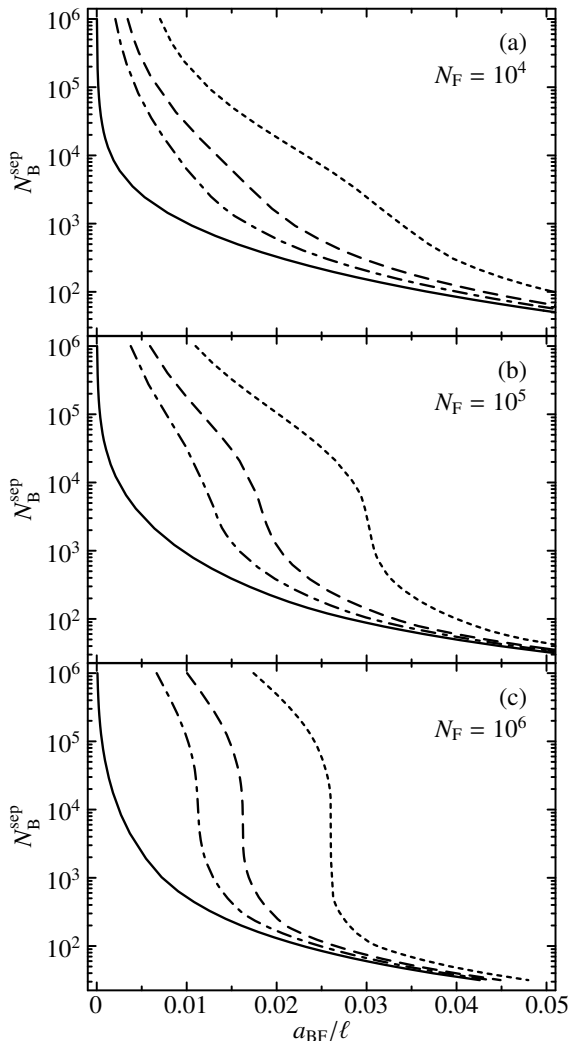
FIG. 6: Characteristic boson number N_B^{sep} for component separation as function of $a_{BF}/\ell > 0$. The curves correspond to different values of the boson-boson scattering length: $a_B/\ell = 0$ (full line), 0.001 (dash-dotted), 0.002 (dashed), 0.005 (dotted). The three panels represent different fermion numbers: (a) $N_F = 10^4$, (b) $N_F = 10^5$, (c) $N_F = 10^6$.

N_B^{sep} is reached, then it drops discontinuously to zero. For a_{BF}/ℓ below the value associated with the step the transition is still continuous which implies the existence of a tricritical point at the step.

C. Collapse of the bosonic component

If the repulsive boson-fermion interaction is supplemented by a boson-boson attraction ($a_B < 0$) then a subtle competition between component separation and mean-field collapse occurs.

For vanishing boson-fermion scattering length $a_{BF} = 0$ the two species decouple. The bosonic component may undergo a mean-field collapse just like an isolated Bose-Einstein condensate if the boson-boson interaction is at-

tractive. The critical particle number for this collapse of the bosonic component in a decoupled mixture can be parameterized by $N_{B,a_{BF}=0}^{cr} = 0.575\,\ell/|a_B|$. This coincides with the result for the collapse a pure Bose gas [20, 24] which was basically confirmed by experiment [25, 26].

One should notice that the character of the collapse induced by a boson-boson attraction differs from that of the collapse cause by an attractive boson-fermion interaction discussed in Sec. III B. In the latter case the boson-fermion interaction generates a mutual attractive mean-field that acts on both, fermions and bosons, and causes a simultaneous collapse of both density distributions. In the case of a boson-boson attraction only the bosonic component experiences an attractive mean-field and may become unstable. For $a_{BF} > 0$ the fermionic density profile will be influenced by a collapse of the bosonic component but it will not collapse itself. The collapse of the bosonic component may, e.g., generate a collective excitation of the fermionic cloud.

Although the collapse for $a_B < 0$ concerns the bosonic density alone, the boson-fermion interaction modifies the stability properties significantly. We will concentrate on the case $a_{BF} > 0$; the collapse in presence of attractive boson-fermion interactions was discussed in Sec. III B already. The black curves in Fig. 7 show the critical number of bosons N_B^{cr} as function of the boson-boson scattering length a_B/ℓ for different values of the boson-fermion scattering length $a_{BF}/\ell \geq 0$. The solid lines show the critical boson numbers for the decoupled mixture ($a_{BF} = 0$).

The first general observation is that a boson-fermion repulsion destabilizes the bosonic component, i.e., the critical boson number N_B^{cr} is reduced if a_{BF}/ℓ or N_F are increased. Physically this can be understood from the structure of the density profiles discussed in Sec. IV A. Due to the boson-fermion repulsion the outer fermionic cloud tends to compress the compact bosonic core. The boson density and thus the attractive mean-field are enhanced which eventually promotes the collapse of the bosonic component. However, as can be seen from Fig. 7 the boson-fermion scattering length a_{BF}/ℓ has to be significantly larger than $|a_B/\ell|$ to have a noticeable effect.

Evidently, component separation due to a boson-fermion repulsion has a large effect on the stability of the mixture with respect to collapse induced by the boson-boson attraction. The gray lines in Fig. 7 indicate the characteristic particle number N_B^{sep} for the onset of component separation for interactions with $a_{BF}/\ell = 0.01$ and 0.02. For weak attractive boson-boson interactions separation happens at lower particle numbers than the collapse of the bosonic component, that is $N_B^{cr} > N_B^{sep}$. With increasing strength of the boson-boson attraction the critical particle number for collapse drops rapidly until $N_B^{cr} = N_B^{sep}$. From that point on collapse and separation happen simultaneously, i.e. there is no stable separated configuration anymore. The corresponding curves for N_B^{cr} shown in Fig. 7 exhibit a kink at this point and proceed towards larger $|a_B/\ell|$ like a smooth continuation

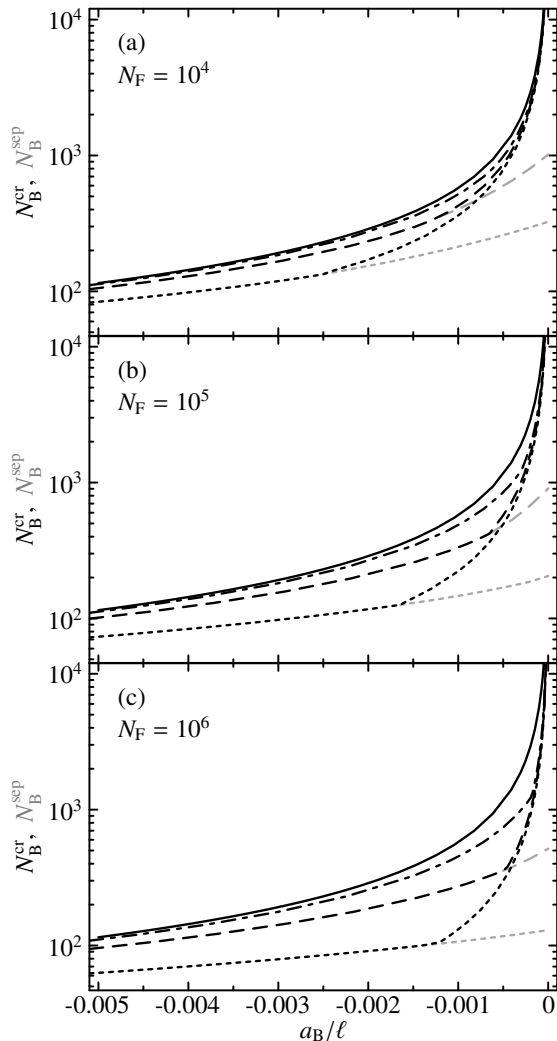FIG. 7: Critical number of bosons $N_{\mathrm{B}}^{\mathrm{cr}}$ above which the bosonic component collapses as function of $a_{\mathrm{B}}/\ell < 0$ (black lines) as well as the characteristic boson number for component separation $N_{\mathrm{B}}^{\mathrm{sep}}$ (gray lines). The curves correspond to different values of the boson-fermion scattering length: $a_{\mathrm{BF}}/\ell = 0$ (full line), 0.005 (dash-dotted), 0.01 (dashed), 0.02 (dotted). The three panels represent different fermion numbers: (a) $N_{\mathrm{F}} = 10^4$, (b) $N_{\mathrm{F}} = 10^5$, (c) $N_{\mathrm{F}} = 10^6$.

of $N_{\mathrm{B}}^{\mathrm{sep}}$. There, as soon as component separation occurs, the bosonic cloud is compressed and the attractive mean-field due to the boson-boson interaction is amplified to such an extent that the collapse happens immediately.

V. IMPLICATIONS FOR PRESENT EXPERIMENTS

After investigating the generic properties of degenerate boson-fermion mixtures in the previous sections I now want to discuss the specific implications for the mixtures available in present experiments. In this section the mass difference and the different oscillator lengths of the trap-

ping potentials for the two species are included explicitly.

A. ^{7}Li-^{6}Li mixture I

Quantum degeneracy in a magnetically trapped dilute boson-fermion mixture was first achieved by Truscott *et al.* [4] using a mixture of bosonic ^{7}Li atoms in the $|F = 2, m_F = 2\rangle$ state and fermionic ^{6}Li with $|F = 3/2, m_F = 3/2\rangle$. The same mixture was subsequently used by Schreck *et al.* [5, 6]. For this particular combination of states the boson-boson interaction is attractive and the boson-fermion interaction repulsive with scattering lengths [27]

$$a_{\mathrm{B}} = -1.46\,\mathrm{nm}\,, \quad a_{\mathrm{BF}} = 2.16\,\mathrm{nm}. \quad (23)$$

The attractive boson-boson interaction can cause the collapse of the bosonic component and leads to a severe limitation of the number of bosons (see Sec. IV C). This is a major hindrance for the implementation of an efficient scheme for the sympathetic cooling of the fermionic component. Ideally one would like to have a large bosonic cloud at a very low temperature to act as a coolant for the fermions. The attractive boson-boson interaction, however, restricts the number of particles in the Bose-Einstein condensate and hence sets a lower bound to the temperature of the bosonic cloud. In conclusion the lowest achievable temperature for the fermionic component is also restricted.

The stability limits for this ^{7}Li-^{6}Li mixture can be visualized by a phase digram in the plane spanned by N_{F} and N_{B} as shown in Fig. 8. Each of the curves marks the limit of stability for a different size of the external trapping potential characterized by the oscillator length ℓ_{B} for the bosonic species. The respective oscillator length ℓ_{F} for the fermions follows from simple scaling with respect to the different masses and magnetic moments. In the experiment of Truscott *et al.* the mean oscillator length is $\ell_{\mathrm{B}} = 2.67\,\mu m$ [4], whereas Schreck *et al.* used a trap with $\ell_{\mathrm{B}} = 1.23\,\mu m$ [5]. For boson numbers above the stability limit the bosonic component is unstable against mean-field collapse. Narrowing of the trapping potential, i.e. reducing the oscillator length ℓ_{B}, enhances the effect of the interactions.

Obviously the stability of the mixture depends mainly on the boson number N_{B} and the critical boson number is to a good approximation given by the corresponding value of the pure Bose gas. The fermionic component has essentially no influence on the stability because the boson-fermion interaction is too weak. This is in agreement with the experimental findings [4, 6]. As discussed in Sec. IV C a stronger boson-fermion repulsion would destabilize the mixture anyway.

Notice that the calculations presented here are restricted to isotropic traps. The prolate trap deformation present in most experiments leads to a reduction of the critical particle number compared to a spherical trap with same mean oscillator length. For a pure Bose gas
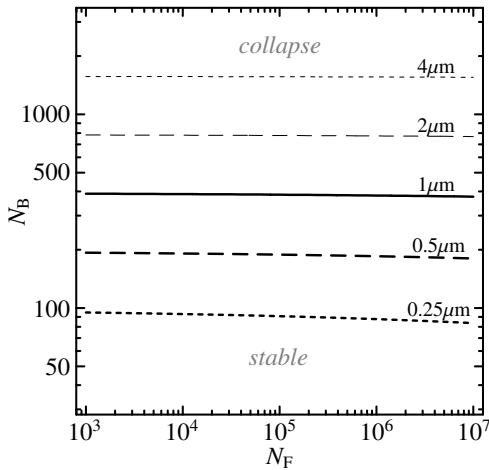
FIG. 8: Phase diagram for a ^{7}Li-^{6}Li mixture with scattering lengths (23). The lines show the stability limit for different values of the oscillator length ℓ_B of the trap as labeled. For N_B above the stability limit the bosonic component collapses.

FIG. 9: Phase diagram for a ^{7}Li-^{6}Li mixture with scattering lengths (24). The lines show the onset of component separation for different values of the oscillator length ℓ_B. For N_B above the limit the two species separate spatially. The gray curve shows the onset of separation for vanishing boson-boson interaction and $\ell_B = 1\mu$m.

in a trap with $\omega_z/\omega_r \approx 0.1$ as in the experiment of Truscott et al. [4] the critical particle number is reduced by typically 20% [28]. For the strongly deformed trap with $\omega_z/\omega_r \approx 0.02$ used by Schreck et al. [5] this reduction is in the order of 40%.

B. ^{7}Li-^{6}Li mixture II

The two Lithium isotopes can also be trapped in another combination of angular momentum states as was successfully demonstrated by Schreck et al. [5]. The relevant s-wave scattering lengths for a mixture of ^{7}Li in the $|F = 1, m_F = -1\rangle$ state and ^{6}Li in $|F = 1/2, m_F = -1/2\rangle$ are both positive [5, 10]

$$a_B = 0.27\,\text{nm}\,, \quad a_{BF} = 2.01\,\text{nm}. \qquad (24)$$

Therefore this mixture is stable with respect to collapse but may undergo component separation generated by the boson-fermion repulsion (see Sec. IV B).

The phase diagram of this mixture in the N_F-N_B-plane is shown in Fig. 9. For values of N_B above the phase boundaries plotted for different oscillator lengths the mixture separates spatially. The onset of separation for the scattering lengths (24) depends in a nontrivial way on the particle numbers and the oscillator length. Especially for tightly confining traps with $\ell_B < 0.15\,\mu$m the phase boundary at large N_F suddenly bends towards smaller boson numbers. As discussed in Sec. IV B this structure is associated with a change in the order of the phase transition. At small N_F or for shallow traps the transition is continuous, i.e. the central fermion density continuously goes to zero as N_B is increased. For large N_F and tightly confining traps the transition is of first order, that is the central fermion density jumps to zero if
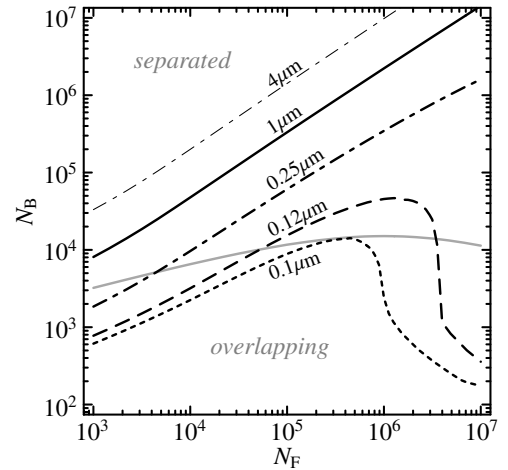
the phase boundary is crossed. This effect is solely caused by the presence of the weak boson-boson repulsion.

We should like to point out that although the boson-boson scattering length is by one order of magnitude smaller than the boson-fermion scattering length it has a strong influence on the phase diagram also for shallow traps and small particle numbers. The gray curve in Fig. 9 shows the phase boundary for $\ell_B = 1\mu$m without the boson-boson interaction (compare with the black solid curve). The boson-boson repulsion stabilizes the system substantially, i.e. the onset of separation is shifted to much larger particle numbers.

Schreck et al. [5] managed to produce such a mixture with $N_B \approx 10^4$ and $N_F \approx 2.5 \times 10^4$ in a trap with mean oscillator length of $\ell_B = 1.0\,\mu$m (solid curve in Fig 9). According to our calculations (effects of the trap anisotropy are not included) the bosonic and fermionic density are still overlapping which is consistent with the experimental findings. However, an increase of the boson number by a factor 10 or a reduction of the fermion number to $N_F \approx 10^3$ would already lead into the regime of separation.

C. ^{87}Rb-^{40}K mixture

A first step towards an ultracold mixture of ^{87}Rb and the fermionic ^{40}K was reported by Goldwin et al. [9] and recently Roati et al. [8] managed to reach quantum degeneracy. This system is particularly interesting, because it shows a large negative boson-fermion scattering length [23]

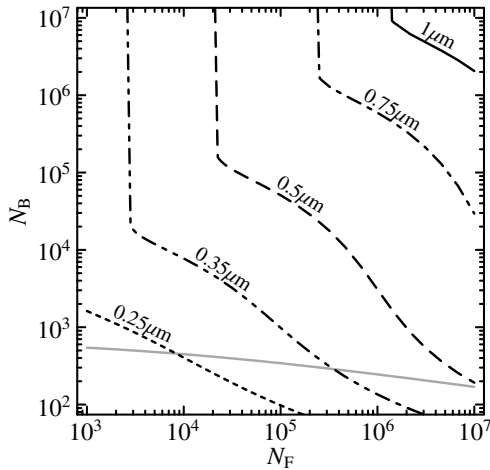$$a_B = 5.25\,\text{nm}\,, \quad a_{BF} = -13.8\,\text{nm}. \qquad (25)$$

FIG. 10: Phase diagram for the ^{87}Rb-^{40}K mixture with scattering lengths (25). The lines show the stability limit for different values of the oscillator length ℓ_B. For N_B above the limit the two species collapse simultaneously. The gray curve shows the stability limit for vanishing boson-boson interaction with $\ell_B = 1\,\mu$m.

Thus this mixture can undergo a simultaneous collapse of the bosonic and fermionic density distribution as discussed in Sec. III B.

Figure 10 shows the corresponding phase diagram in the N_F-N_B-plane. One might expect that the strong boson-fermion attraction sets a very severe limit to the size of a stable mixture. In principle this expectation is correct as illustrated by the gray solid curve which corresponds to the mere boson-fermion attraction for $\ell_B = 1\,\mu$m. Without the boson-boson interaction the mixture would collapse if the boson number exceeds $N_B^{cr} \approx 300$.

Fortunately a moderate repulsive boson-boson interaction is present which has a tremendous influence on the phase diagram. First of all the critical boson numbers are increased by roughly four orders of magnitude. Moreover, below a certain fermion number marked by the vertical pieces of the curves in Fig. 10 the mixture is stable up to arbitrary boson numbers; this is the effect of absolute stabilization due to the boson-boson repulsion discussed in Sec. III B. Thus in a trap with $\ell_B = 1\,\mu$m any combination of boson and fermion numbers up to $N_B \approx N_F \approx 10^7$ would be stable although a strongly attractive boson-fermion interaction is present.

The particular combination of scattering lengths of the ^{87}Rb-^{40}K mixture opens interesting perspectives for the implementation of a sympathetic cooling scheme. The strong boson-fermion attraction generates an enhancement of the boson and fermion density in the overlap region which is — due to the boson-boson repulsion — expanded over a large volume (see Fig. 2). Therefore a large fraction of the fermionic cloud overlaps with the bosonic distribution and enables a very efficient interspecies thermalization. At the same time the boson-boson repulsion stabilizes the system against simultaneous collapse for all experimentally relevant particle numbers.

D. ^{23}Na-^{6}Li mixture

Recently, Hadzibabic et al. [7] reported the sympathetic cooling of a mixture of ^{23}Na and ^{6}Li to quantum degeneracy. To my knowledge there is no data on the inter-species scattering length for this system yet. However, since a stable mixture with large numbers of bosons and fermions ($N_B \approx 2 \times 10^6$, $N_F =\approx 1.5 \times 10^5$) was produced one can at least deduce bounds for the boson-fermion scattering length. Assuming $a_B = 2.75$ nm [29] one finds that the boson-fermion scattering length must obey $a_{BF} > -14.6$ nm in order to allow a stable mixture in this experiment. Moreover, the linear density profiles of the fermionic cloud shown in [7] suggest that the components are not separated. From the minimal requirement that the fermion density in the center is larger than zero one obtains an upper bound $a_{BF} < 5.1$ nm [30]. Notice that these estimates do not account for the effects of the trap anisotropy and the finite temperature present in the experiment.

VI. CONCLUSIONS

In summary, I have presented a systematic study of the structure and stability of trapped binary boson-fermion mixtures at zero temperature. The bosonic component is described by a modified Gross-Pitaevskii equation which includes the mean-field interaction with the fermionic component. The fermionic density distribution is obtained within the Thomas-Fermi approximation.

Depending on the strengths of the boson-boson and the boson-fermion interactions, characterized by the s-wave scattering lengths a_B and a_{BF}, respectively, different structural phenomena can be observed:

$a_B < 0$: The collapse of the bosonic component dominates the phase diagram and sets a severe limitation to the maximum number of bosons in a stable mixture. The boson-fermion interaction has only small influence, however, attractive as well as repulsive boson-fermion interactions promote the collapse of the bosonic component.

$a_B \geq 0, a_{BF} < 0$: The boson-fermion attraction enhances the density of both species in the overlap region and can cause a simultaneous collapse of the bosonic and the fermionic cloud. A repulsive boson-boson interaction stabilizes the system, i.e. increases the critical particle numbers.

$a_B \geq 0, a_{BF} > 0$: Repulsive boson-fermion interactions reduce the overlap of the two species and eventually lead to the spatial separation of the components.

Again a repulsive boson-boson interaction stabilizes the mixture against separation.

The rich variety of structures generated by the interplay of boson-boson and boson-fermion interactions has important consequences for the experimental realization of sympathetic cooling schemes. As far as the density distributions are concerned efficient sympathetic cooling relies on (a) the mechanical stability of the mixture and (b) a large overlap of the two species.

From this point of view mixtures with repulsive boson-boson interactions ($a_B > 0$) are superior since they do not suffer the severe limitation of the boson number imposed by the collapse for $a_B < 0$. The boson-fermion cross section and thus the modulus of the boson-fermion scattering length should be sufficiently large to enable efficient inter-species thermalization. For $a_{BF} > 0$ this may lead into problems with the separation of the two components, for $a_{BF} < 0$ there may be a simultaneous collapse of both clouds. Fortunately, a moderate boson-boson repulsion can stabilize the mixture against both transitions.

Regarding the structure of the density profiles a mixture with $a_B > 0$ and $a_{BF} < 0$ — like the ^{87}Rb-^{40}K mixture discussed in Sec. V C — is especially appealing for the implementation of an efficient sympathetic cooling scheme. It is stabilized against collapse by the boson-boson repulsion and exhibits a large overlap between the species due to an extended boson distribution and a significantly increased fermion density within the overlap volume.

[1] M. Inguscio, S. Stringari, and C. Wieman, eds., *Proceedings of the International School of Physics "Enrico Fermi" on Bose-Einstein condensation in Varenna 1998* (ISO Press, Amsterdam, 1999).

[2] B. DeMarco and D. S. Jin, Science **285**, 1703 (1999).

[3] S. R. Granade, M. E. Gehm, K. M. O'Hara, and J. E. Thomas (2001), cond-mat/0111344.

[4] A. G. Truscott, K. E. Strecker, W. I. McAlexander, G. B. Partridge, and R. G. Hulet, Science **291**, 2570 (2001).

[5] F. Schreck, L. Khaykovich, K. L. Corwin, G. Ferrari, T. Bourdel, J. Cubizolles, and C. Salomon, Phys. Rev. Lett. **87**, 080403 (2001).

[6] F. Schreck, G. Ferrari, K. L. Corwin, J. Cubizolles, L. Khaykovich, M.-O. Mewes, and C. Salomon, Phys. Rev. A **64**, 011402 (2001).

[7] Z. Hadzibabic, C. A. Stan, K. Dieckmann, S. Gupta, M. W. Zwierlein, A. Görlitz, and W. Ketterle (2001), cond-mat/0112425.

[8] G. Roati, F. Riboli, G. Modugno, and M. Inguscio (2002), cond-mat/0205015.

[9] J. Goldwin, S. B. Papp, B. DeMarco, and D. S. Jin, Phys. Rev. A **65**, 021402(R) (2002).

[10] F. A. vanAbeelen, B. J. Verhaar, and A. J. Moerdijk, Phys. Rev. A **55**, 4377 (1997).

[11] R. Roth and H. Feldmeier, Phys. Rev. A **65**, 021603(R) (2002).

[12] K. Mølmer, Phys. Rev. Lett. **80**, 1804 (1998).

[13] Z. Akdeniz, P. Vignolo, A. Minguzzi, and M. P. Tosi, J. Phys. B **35**, L105 (2002).

[14] T. Miyakawa, T. Suzuki, and H. Yabu, Phys. Rev. A **64**, 033611 (2001).

[15] M. Amoruso, C. Minniti, and M. P. Tosi, Eur. Phys. J. D **8**, 19 (1999).

[16] N. Nygaard and K. Mølmer, Phys. Rev. A **59**, 2974 (1999).

[17] R. Roth and H. Feldmeier, Phys. Rev. A **64**, 043603 (2001).

[18] R. Roth and H. Feldmeier, J. Phys. B **34**, 4629 (2001).

[19] J. L. Bohn, Phys. Rev. A **61**, 053409 (2000).

[20] F. Dalfovo, S. Giorgini, L. P. Pitaevskii, and S. Stringari, Rev. Mod. Phys. **71**, 463 (1999).

[21] P. Ring and P. Schuck, *The Nuclear Many-Body Problem* (Springer Verlag, New York, 1980).

[22] M. F. Feagin, *Quantum Methods with Mathematica* (Springer Verlag, New York, 1994).

[23] G. Ferrari, M. Inguscio, W. Jastrzebski, G. Modugno, G. Roati, and A. Simoni (2002), cond-mat/0202290.

[24] A. Eleftheriou and K. Huang, Phys. Rev. A **61**, 043601 (2000).

[25] J. L. Roberts, N. R. Claussen, S. L. Cornish, E. A. Donley, E. A. Cornell, and C. E. Wieman, Phys. Rev. Lett. **86**, 4211 (2001).

[26] C. C. Bradley, C. A. Sackett, and R. G. Hulet, Phys. Rev. Lett. **78**, 985 (1997).

[27] E. R. I. Abraham, W. I. McAlexander, J. M. Gerton, R. G. Hulet, R. Cote, and A. Dalgarno, Phys. Rev. A **55**, R3299 (1997).

[28] A. Gammal, T. Frederico, and L. Tomio, Phys. Rev. A **64**, 055602 (2001).

[29] S. Inouye, M. R. Andrews, J. Stenger, H.-J. Miesner, D. M. Stamper-Kurn, and W. Ketterle, Nature **392**, 151 (1998).

[30] The requirement that the fermionic density profile drops monotonically, i.e. does not show a central dip, leads to the more restrictive upper bound $a_{BF} < 0.69 \, \text{nm}$.